Stability and State of Aggregation of Aqueous Fibrinogen and Dipalmitoylphosphatidylcholine Lipid Vesicles

Sook Heun Kim,† Lilac Haimovich-Caspi,‡ Liora Omer,‡ Chi-Ming Yu,† Yeshayahu Talmon,‡ Nien-Hwa Linda Wang,† and Elias I. Franses*,†

School of Chemical Engineering, Purdue University, 480 Stadium Mall Drive, West Lafayette, Indiana 47907-2100, and Department of Chemical Engineering, Technion-Israel Institute of Technology, Haifa 32000, Israel

Received November 29, 2006. In Final Form: February 27, 2007

The stability and state of aggregation of aqueous fibrinogen (FB) and dipalmitoylphosphatidylcholine (DPPC) vesicles in water or buffer at 25 °C were studied with dynamic light scattering (DLS), UV−vis spectroturbidimetry (ST), and cryo-transmission electron microscopy (cryo-TEM). In water, when 1000 ppm (0.10 wt %) DPPC dispersions were prepared with a protocol including extensive sonication, they contained mostly vesicles and were quite clear, transparent, and stable for at least 30 days. FB mixtures with water (0.075 wt %) were quite unstable and biphasic. They formed large aggregates which eventually precipitated. The addition of DPPC vesicles into these unstable FB dispersions reversed FB aggregation and precipitation and produced stable translucent microdispersions. The inferred lipid/protein aggregates were limited in size, with average diameters ranging from 200 to 300 nm. In buffer, DPPC dispersions were also clear and quite stable, with average dispersed particles diameter of ca. 90 nm. FB dissolved in aqueous buffer and formed transparent and stable solutions. Adding salt to an aggregated FB dispersion in water reversed the aggregation. FB aggregated and redissolved in the presence of the citrate and after the citrate was removed. There was no effect of citrate (present in FB initially) in the FB aggregation or redissolution. FB molecules in buffer form dimers or higher aggregates. Their average aggregation number is 2, determined with Rayleigh scattering analysis of turbidity data. The average hydrodynamic diameter of FB solutions from DLS was 30 nm. Mixing a stable FB solution in buffer and a stable DPPC dispersion in buffer produced highly unstable mixtures, in which large aggregates precipitated. These results have implications in understanding the interactions of lipids and proteins in many biological applications and food processing applications.

1. Introduction

The interactions of proteins and lipids are important in many biological applications, such as biosensors,[1,2] cell membranes, lung surfactants,[3] in food processing applications, and in emulsion formation and stabilization.[4,5] Dipalmitoylphosphatidylcholine (DPPC) is the major component of natural lung surfactant, which stabilizes the lung alveoli by reducing the dynamic surface tension (DST) at the air/aqueous interface and helps maintain the lung alveoli healthy.[3,6] The sizes of DPPC particles, liposomes, or vesicles, can vary from several micrometers to ∼20 nm depending on the protocol of the dispersion preparation.[3,7−12] For DPPC particles in water or buffer, the effect of the protocol of preparation has been studied, and cases were found (including extensive sonication) whereby very low DST's, lower than 1 mN/m, were observed.[13,14] We discovered a protocol in which the sonicated DPPC dispersions contained mostly frozen vesicles with nearly spherical and nearly polyhedral shapes and were quite clear, transparent, and stable for at least 30 days.[15]

Fibrinogen (FB) glycoprotein is found in the blood plasma of vertebrate animals. FB is produced in the liver and can contribute to stopping bleeding by helping blood clots to form along with platelets. FB can be broken down into short fragments of fibrin by the enzyme thrombin. FB is composed of two identical subunits, each containing three dissimilar polypeptide chains (α, β, γ) which are linked by disulfide bonds. Following numerous studies, the FB molecular structure and conformation are well known.[16−23] Shadow-cast electron microscope images by Hall and Slayter revealed a triglobular structure ∼47 nm in length.[16] Its subdomainal structure has been also visualized by

* To whom correspondence should be addressed. Phone: (765) 494-4078. Fax: (765) 494-0805. E-mail: franses@ecn.purdue.edu.

† Purdue University.

‡ Technion-Israel Institute of Technology.

(1) Zhu, D. G.; Petty, M. C.; Ancelin, H. H.; Yarwood, J. *Thin Solid Films.* **1989**, *176*, 151.

(2) Okahata, O.; Tsuruta, T.; Ijiro, K.; Ariga, K. *Thin Solid Films.* **1989**, *180*, 65.

(3) Notter, R. H. *Lung Surfactants*; Marcel Dekker: New York, 2000.

(4) Darling, D. F.; Birkett, R. J. In *Food Emulsions and Foams*; Dickinson, E., Ed.; Royal Society of Chemistry: London, 1986; Chapter 1, pp 1−29.

(5) Dickinson, E.; Stainsby, G. *Colloids in Food*; Applied Science: London, 1982; Chapter 1, pp 1−9.

(6) Shapiro, D. L. In *Surfactant Replacement Therapy*; Shapiro, D. L., Notter, R. H., Eds.; Alan R. Liss, Inc.: New York, 1989; pp 1−17.

(7) Wen, X.; Franses, E. I. *Langmuir* **2001**, *17*, 3194.

(8) Szoka, F. *Annu. Rev. Biophys. Bioeng.* **1980**, *9*, 467.

(9) Hope, M. J.; Bally, M. B.; Mayer, L. D.; Janoff, A. S.; Cullis, P. R. *Chem. Phys. Lipids* **1986**, *40*, 89.

(10) Park, S. Y. Ph.D. Thesis, Purdue University, West Lafayette, IN. 1995.

(11) Park, S. Y.; Franses, E. I. *Langmuir* **1995**, *11*, 2187.

(12) Park, S. Y.; Perk, S. C.; Chang, C. H.; Franses, E. I. In *Dynamic Properties of Interfaces and Association structures*; Shah, D. O., Ed.; American Oil Chemists Society: Champaign, IL, 1996.

(13) Kim, S. H.; Franses, E. I. *J. Colloid Interface Sci.* **2006**, *295*, 84.

(14) Kim, S. H.; Franses, E. I. *Colloid Surf., B.* **2005**, *43*, 256.

(15) Kim, S. H.; Haimovich-Caspi, L.; Omer, L.; Talmon, Y.; Franses, E. I. *J. Colloid Interface Sci.* **2007**, in press.

(16) Hall, C. E.; Slayter, H. S. *J. Biophys. Biochem. Cytol.* **1959**, *5*, 11.

(17) Willams, R. C. *J. Mol. Biol.* **1981**, *150*, 399.

(18) Rao, S. P.; Poojary, M. D.; Elliott, B. W.; Melanson, L. A.; Oriel, B.; Cohen, C. *J. Mol. Biol.* **1991**, *222*, 89.

(19) Yee, V. C.; Pratt, K. P.; Cote, H. C.; LeTrong, I.; Chung, D. W.; Davie, E. W.; Stenkamp, R. E.; Teller, D. *Structure* (London), **1997**, *5*, 125.

(20) Spraggon, G.; Everse, S. J.; Doolittle, R. F. *Nature* (London), **1997**, *389*, 455.

(21) Everse, S. J.; Spraggon, G.; Veerapandian, L.; Riley, M.; Doolittle, R. F. *Biochemistry* **1998**, *37*, 8637.

(22) Everse, S. J.; Spraggon, G.; Veerapandian, L.; Doolittle, R. F. *Biochemistry* **1999**, *38*, 2941.

(23) Yang, Z.; Mochalkin, I.; Veerapandian, L.; Riley, M.; Doolittle, R. F. *Biochemistry* **2000**, *97*, 3907.

10.1021/la0634701 CCC: $37.00
Published on Web 04/05/2007

negative staining electron microscopy and determined by low-resolution X-ray crystallography.[17,18] The crystal structure of FB was also reported.[19−23] Nonetheless, little work has been reported on the state of FB in aqueous solution. In this article we report dynamic light scattering (DLS), spectroturbidimetry (ST), and cryogenic-temperature transmission electron microscopy (cryo-TEM) results on the state of aggregation of FB in solution.

FB has a molecular weight of 340 kDa (for the two subunits mentioned above) and equivalent spheroidal semiaxes dimensions of $2.5 \times 2.5 \times 23$ nm.[24] FB is quite surface active at the air/water interface; it can decrease the DST to ~50 mN/m quite rapidly. When FB is secreted into the alveolar lining layer due to alveolar stress or lung injury, it can inhibit the lung surfactant DST lowering function and can be a contributing cause of the Adult or Acute Respiratory Distress Syndrome (ARDS).[3] In addition to reported interfacial interactions,[13,14,25−35] there have been several reports about the interactions of serum proteins (FB or bovine serum albumin) with DPPC or other lipids in aqueous solution.[36−44] Thus, understanding interactions of FB with DPPC and other lipids may have impact in elucidating the etiology and possible treatment strategies for alveolar respiratory diseases. It is known that when DPPC monolayers are prepared on an aqueous surface, no protein (BSA or FB) injected in solution is adsorbed.[13,14] When protein is preadsorbed on the air/water interface, no DPPC vesicles adsorb. Therefore, FB and DPPC do not bind at the air/water interface. This has been shown by IRRAS experiments, supplemented by ellipsometry results.[13,14] The interactions of DPPC vesicles with protein in the bulk are of particular interest in this article. The interactions of FB with DPPC vesicles are important for lung-surfactant-related applications detailed above, potentially important in assessing the lifetime and clearance of liposomes in the bloodstream,[45−47] and in the mechanism of formation of atheromatous plaque containing FB, lipids, and other blood components.[48−50] In the present study, we use DLS, UV−vis spectroturbidimetry, and cryo-TEM to probe for aggregation of FB with DPPC vesicles.

2. Materials and Methods

2.1. Materials. Synthetic L-α-dipalmitoylphosphatidylcholine (DPPC, 99% pure) and FB (type I-S: from bovine plasma) were purchased from Sigma Chemical Co. (St. Louis, MO). The FB, in powder form, contains 75 wt % FB, 15 wt % sodium chloride, and 10 wt % sodium citrate, used in the isolation and stabilization of the protein. Sodium chloride (NaCl) and sodium dihydrogen phosphate ($NaH_2PO_4 \cdot H_2O$) were purchased from Mallinckrodt Specialty Chemicals Co. (Paris, KY). Disodium hydrogen phosphate dodecahydrate ($Na_2HPO_4 \cdot 12H_2O$) was purchased from Fluka Chemical Corp. (Milwaukee, WI). All materials were used as received. The lipid dispersions and the protein solutions were prepared on a weight basis. Standard phosphate buffer saline or "buffer", of 150 mM NaCl, 32 mM $NaH_2PO_4 \cdot H_2O$, and 93 mM $Na_2HPO_4 \cdot 12H_2O$, was used. Water was first distilled and then passed through a Millipore four-stage cartridge system; it had a resistivity of 18 MΩ·cm at the exit port.

2.2. Protocols for Preparation of Vesicular DPPC Dispersions and FB Solution. DPPC dispersions (1000 ppm) were prepared by a special protocol that leads to stable vesicles: the sample is first heated for 30 min at 55−60 °C (above T_c); then, the dispersion is stirred with a magnetic stirrer for 1 h to form primarily dispersions of fluid liposomes. These dispersions are sonicated extensively at 55 °C in a sonicator bath (for about 7 h), until they are completely clear and transparent, with no particles visible by eye or in the optical microscope, for producing dispersions containing primarily fluid vesicles. Finally, the dispersions are cooled to 25 °C (below T_c). The sonicator bath (Branson 3510 Ultrasonic cleaner, Branson Cleaning Equipment Co., Shelton, CT) has a maximum input power of 130 W and a nominal frequency of 40 kHz. These preparation protocol methods were originally described in ref 13.

FB solutions were prepared with magnetic stirring for 20 min at 25 °C. In buffer, this procedure leads to a clear, stable solution (see Section 3.1). In water, this procedure leads to aggregates. To examine the possible effect of the citrate on the FB solution stability, an FB solution of 750 ppm was dialyzed using a cellulose ester dialysis membrane with a MW cutoff of 1000. As detailed in Section 3.1, the FB aggregated/precipitated even faster than before the dialysis. For FB/DPPC mixtures, a freshly prepared FB solution and a sonicated DPPC dispersion were mixed with gentle stirring. The pH values of the DPPC dispersions, the FB solutions, and the FB/DPPC mixtures in buffer were from 7.0 to 7.2. The pH of the FB solution in water was 8.2, probably because of the influence of sodium citrate. The pH of the FB/DPPC mixture in water was 7.4. To examine the reversibility of aggregation, an FB solution in buffer was also prepared with the following order of mixing. First, the FB was dissolved in water, and then the salt/phosphates were added to form the buffer. For a test of the citrate effect and the reversibility of aggregation, an FB solution was prepared in water, dialyzed for 24 h, and then the salts were added. As detailed in Section 3.1, the resulting solutions were all clear.

2.3. DLS Measurements. Size distribution analysis of DPPC dispersions, FB solutions, and their mixtures in water or buffer at 25 °C was performed with a Brookhaven ZetaPALS dynamic light scattering instrument, which had a BI-9000AT digital autocorrelator at 659 nm wavelength. Standard square 4.5 mL cuvettes were used. Each measurement usually took about 2 min. Three measurements were taken for each system and then averaged.

The available software uses the relaxation rate, Γ, at a given scattering vector $q = (4\pi n_s/\lambda)\sin(\theta/2)$ to obtain the mean translational diffusion coefficient D, from which the hydrodynamic diameter $d_h = 2R_h$ is obtained. In addition, the half width of the distribution

(24) Armstrong, J. K.; Wenby, R. B.; Meiselman, H. J.; Fisher, T. C. *Biophys. J.* **2004**, *87*, 4259.
(25) Teneva, S.; Panaiotov, I.; Ter-Minassian-Saraga, L. *Colloids Surf.* **1984**, *10*, 101.
(26) Seeger, W.; Stohr, G.; Wolf, H. R. D.; Neujof, H. *J. Appl. Physiol.* **1985**, *58*, 326.
(27) Fuchimukai, T.; Fujiwara, T.; Takahashi, A.; Enhorning, G. *J. Appl. Physiol.* **1987**, *62*, 429.
(28) Patino, J. M. R.; Nino, M. P. R. *Colloids Surf., A* **1995**, *103*, 91.
(29) Cho, D.; Narsimhan, F.; Franses, E. I. *Langmuir* **1997**, *13*, 4710.
(30) Cheng, C. C.; Chang, C. H. *Langmuir* **2000**, *17*, 437.
(31) Hernandez, E. M.; Phang, T. Z.; Wen, X.; Franses, E. I. *J. Colloid Interface Sci.* **2002**, *250*, 271.
(32) Liu, Y.-L.; Chang, C.-H. *Colloid Polym. Sci.* **2002**, *280*, 683.
(33) McClellan, S. J.; Franses, E. I. *Colloids Surf., B* **2003**, *30*, 1.
(34) Phang, T. L.; Frnases, E. I. *J. Colloid Interface Sci.* **2004**, *275*, 477.
(35) Phang, T. L.; McClellan, S. J.; Franses, E. I. *Langmuir* **2005**, *21*, 10140.
(36) Parise, L. V.; Phillips, D. R. *J. Biol. Chem.* **1985**, *260*, 10698.
(37) Bonté, F.; Juliano, R. L. *Chem. Phys. Lipids* **1986**, *40*, 359.
(38) Jones, M. N.; Nicholas, A. R. *Biochim. Biophys. Acta* **1991**, *1065*, 145.
(39) Cserhati, T.; Szogyi, M. *Int. J. Biochem.* **1993**, 25, 123.
(40) Gunther, A.; Bleyl, H.; Seeger, W. *Am. J. Physiol. Lung Cell Mol. Physiol.* **1993**, *265*, 186.
(41) Gunther, A.; Kalinowski, M.; Elssner, A.; Seeger, W. *Am. J. Physiol. Lung Cell Mol. Physiol.* **1994**, *267*, 618.
(42) Cunningham, B. A.; Kücük, Ö.; Kwaan, H. C.; Westerman, M. P.; Tracy, D.; Lis, L. J. *Chem. Phys. Lipids* **1994**, *72*, 1.
(43) Cunningham, M. T.; Citron, B. A.; Koerner, T. A. W. *Thromb. Res.* **1999**, *95*, 325.
(44) Galánti, R.; Bárdos-Nagy, I. *Int. J. Pharm.* **2000**, *195*, 207.
(45) Senior, J.; Delgado, C.; Fisher, D.; Tilcock, C.; Gregoriadis, G. *Biochim. Biophys. Acta* **1991**, *1062*, 77.
(46) Lasic, D. D.; Needham, D. *Chem. Rev.* **1995**, *95*, 2601.
(47) Price, M. E.; Cornelius, R. M.; Brash, J. L. *Biochim. Biophys. Acta* **2001**, *1512*, 191.
(48) Retzinger, G. S. *Arterioscler. Thromb.* **1995**, *15*, 786.
(49) Kunz, F.; Pechlaner, C.; Erhart, R.; Zwierzina, W-D.; Kemmler, G. *Arterioscler. Thromb.* **1992**, *12*, 1516.
(50) Fatah, K.; Hamsten, A.; Blombäck, B.; Blombäck, M. *Thromb. Haemost.* **1992**, *68*, 130.

of d_h is also calculated. The relevant equation is

$$D = \Gamma/q^2 \tag{1}$$

where n_s is the refractive index of the solution, λ is the wavelength of the radiation in vacuum, and θ is the scattering angle; $\theta = 90°$ was used. The apparent hydrodynamic radius, R_h, is found from the Stokes−Einstein equation,

$$R_h = k_B T/6\pi\eta D \tag{2}$$

where k_B is the Boltzmann constant, T is the absolute temperature, and η is the solvent viscosity. This equation is valid for rigid spherical particles in a Newtonian liquid with a no-slip boundary condition.[51] Any possible particle hydration is included in R_h. The presumed Gaussian distribution of the particle sizes is calculated by using the measured average d_h (d_{av}) and half width from each measurement. The range of the diameters (d_{range}) was taken from this calculated Gaussian distribution for sizes between 10% and 90% of the total distribution, also using a constraint of 5 nm for the lowest minimum value.

If the particles are spherical with a radius R, then one takes $R_h \cong R$. For the nonspherical FB molecule, and for FB−DPPC aggregates, R_h may depend on the particle shape and overall dimensions. If the FB molecule can be approximated as a rigid prolate spheroid, with semiaxes dimensions $b \times b \times a = 2.5 \times 2.5 \times 23$ nm, then from Perrin's equation,[52]

$$d_h = 2\frac{(a^2 - b^2)^{1/2}}{\ln\left(\frac{a + (a^2 - b^2)^{1/2}}{b}\right)} \tag{3}$$

one finds $d_h = 16$ nm. If the FB molecule is approximated as a cylinder with radius $R = 2.5$ nm and length $L = 46$ nm, d_h is found from the following equation,[53,54]

$$d_h = L\frac{1}{\bar{s}} \tag{4}$$

where

$$\bar{s} = \ln\left(\frac{L}{R} + \left(\frac{L^2}{R^2} + 1\right)^{1/2}\right) - \frac{R}{L}\left(\frac{L^2}{R^2} + 1\right)^{1/2} + \frac{R}{L} \tag{4a}$$

then, one finds $d_h = 18$ nm.[24] These estimates will be compared to the results from the DLS data.

2.4. UV−Vis Spectroturbidimetry. A DU 520 UV−vis spectrophotometer (Beckman Coulter, Inc., Fullerton, CA) was used at wavelengths from 600 to 250 nm for probing the dispersion stability from the absorbance changes and for estimating the particle sizes. Standard cells of 1 cm path length were used. Because generally smooth spectra were obtained in this range,[55] only the absorbances (A) at 500 and 380 nm are reported. The wavelength exponent, g, from the equation $A \propto \lambda_o^{-g}$ was calculated from these two wavelengths. The average particle sizes were estimated using Mie's theory and the Heller et al. method and tables,[56] which are valid for uniform-size (monodisperse) compact spheres, for an estimated refractive index ratio of $m = n_p/n_w = 1.10$. This method is less accurate than the method using absolute absorbances, but it does not rely on knowing the exact values of the particles volume fraction and the exact vesicle effective (average) refractive index, which may be affected by the water content of the vesicles. Other errors in the method may result from using the Mie equations, which are strictly valid for monodisperse compact spheres, to polydisperse, noncompact, and slightly nonspherical particles. Nonetheless, the results of this method, albeit approximate, provide a fast and convenient estimate of the particle size and are generally consistent with those from DLS, as shown below.

Light scattering is a well-known technique for measuring the apparent average molecular weight of polymers and proteins.[57] When intraparticle interference is negligible and the particles are small compared to the wavelength λ (i.e., $d \leq \lambda/20$), then the scattering is called Rayleigh scattering. At these conditions, the intensity of the scattered light is proportional to λ^{-4} and independent of the scattering angle. One can calculate the turbidity, τ, from measurements of the scattered intensity and determine the apparent weight-average molecular weight, M, and the second virial coefficient, B, from the following equation:

$$\frac{Hc}{\tau l} = \frac{1}{M} + 2Bc \tag{5}$$

where c (g/mL) is the solute concentration, τ (cm^{-1}) is the turbidity per unit path length, l (cm) is the path length, H is the optical constant (cm^2/g^2), defined as

$$H = \frac{32\pi^3 n^2 \left(\frac{dn}{dc}\right)^2}{3N_A\lambda^4} \tag{6}$$

n is the solution refractive index, dn/dc is the refractive index increment of the solute; for proteins dn/dc = 0.186;[58] N_A is Avogadro's number, $\lambda = \lambda_0/n_0$, where λ_0 is the wavelength of incident light in vacuum, and n_0 is the refractive index of the medium, which is in the range from 1.333 to 1.331 for the solvents used here.[59]

Instead of measuring the turbidity, τ, from the angular dependence of the scattering intensity at one wavelength, one can also determine τ from absorbance (A) measurements at wavelengths $\lambda > 350$ nm, where light absorption is negligible. This method was found in a recent paper by three of the current authors to be quite sensitive and effective to determine the molecular weight of insulin aggregates.[60] Using a photodiode array (PDA) detector, which is commonly available in chromatographic apparatus, one can obtain the spectrum from 400 to 200 nm. The absorbances from 400 to 350 nm are used to determine the wavelength dependence and confirm that scattering falls in the Rayleigh regime. The absorbance at one wavelength, here at 390 nm, is then adequate for determining the turbidity, τ, from A as follows

$$\tau l = -\ln\left(\frac{I_0 - I_s}{I_0}\right) = -\ln\left(1 - \frac{I_s}{I_0}\right) = 2.303A \tag{7}$$

where I_0 is the intensity of the incident light and I_s is the total intensity of all the scattered light. Calculations at other wavelengths in the nonabsorbing range may also be used, if needed, for consistency tests. The absorbance at the absorption peak, at ~280 nm, was also used to ascertain the protein concentration.

A Waters 996 PDA detector was used to measure absorbances in the range from 10^{-5} to 2 AU. The feed pump was a Series 200 Perkin-Elmer pump. The source was a UV lamp. At the lower absorbance ranges used, the precision can be typically ±0.00002 AU, which allows reliable absorbance measurements for AU ≥ 0.0001. A Waters Millennium software operating in the Windows environment was used for data collection and analysis.

Samples of 20 mL were directly injected into the detectors with a Perkin-Elmer pump at a flow rate of 2 mL/min. A series of step

(51) Berne, B. J.; Pecora, R. *Dynamic Light Scattering with Application to Chemistry, Biology, and Physics*; Mineola: New York, 2000.
(52) Perrin, F. *J. Phys. Radium* **1936**, *7*, 1.
(53) Yoshizaki, T.; Yamakawa, H. *J. Chem. Phys.* **1980**, *72*, 57.
(54) He, L.; Niemeyer, B. *Biotechnol. Prog.* **2003**, *19*, 544.
(55) Kim, S. H. Ph.D. Thesis, Purdue University, expected in 2007.
(56) Heller, W.; Bhatnagar, H. L.; Nakagaki, M. *J. Chem. Phys.* **1962**, *36*, 1163.
(57) Hiemenz, P. C.; Rajagopalan, R. *Principles of Colloid and Surface Chemistry*; Marcel Dekker: New York, 1997.
(58) Whittingham, J. L.; Scott, D. J.; Dodson, G. G. *J. Mol. Biol.* **2002**, *318*, 479.
(59) Weast R. C., Ed. *CRC Handbook of Chemistry and Physics*; CRC Press: Boca Raton, FL, 1980.
(60) Yu, C. M.; Chin, C. Y.; Franses, E. I.; Wang, N. H. L. *J. Colloid Interface Sci.* **2006**, *299*, 733.

Table 1. Average Diameter (d_{av}) and the Range of the Diameters (d_{range}) of FB and FB/DPPC Mixture Particles in Water or in Buffer at 25 °C

	750 ppm FB		750 ppm FB/ 1000 ppm DPPC	
time, days	d_{av}[a], nm	d_{range}[b], nm	d_{av}[a], nm	d_{range}[b], nm
		In Water		
0[c]	783 ± 26	20−1550	263 ± 32	10−520
0.1	803 ± 37	5−2070	213 ± 25	20−410
2	1213 ± 81[d]	5−2450	241 ± 66	50−430
9	1804 ± 76[d]	1020−2590	N/A	N/A
16	1813 ± 264[d]	1580−2040	281 ± 20	5−560
23	1651 ± 160[d]	5−3550	238 ± 5	5−470
30	1511 ± 520[d]	5−3150	224 ± 6	20−430
		In Buffer		
0[c]	61 ± 1	5−133	160 ± 2	10−310
2	34 ± 8	5−73	423 ± 18	5−850
9	30 ± 1	7−52	738 ± 85	5−1530
16	32 ± 5	5−57	851 ± 23[d]	5−1830
23	30 ± 2	7−53	1617 ± 432[d]	5−3200
33	34 ± 10	5−63	2003 ± 486[d]	5−4000

[a] Average diameter with three measurements. [b] Range of the diameters taken from the calculated Gaussian distribution of the sizes between 10% and 90% of the total distribution; see Figure 1. [c] Measurements were taken for the freshly prepared sample within 0.5 h. [d] Some material flocculated and settled; sample was shaken and homogenized before each measurement.

changes in solution concentration were done at, 20 and 37 °C, with concentrations of 0.75, 0.563, 0.375, 0.188, and 0.075 g/L.

2.5. Cryo-TEM. Cryo-TEM vitrified specimens were prepared in a controlled environment vitrification system (CEVS).[61] All solutions were quenched from 100% relative humidity and the desired temperature by plunging into liquid ethane at its freezing point. Specimens were examined either in a Philips CM120 microscope, using an Oxford CT-3500 cryo-holder system, or an FEI T12 G2 microscope, using a Gatan 626 cryo-holder system. All specimens were kept below −178 °C and observed with 120 kV electrons. Images were recorded digitally in the minimal electron dose mode by a Gatan 791 MultiScan (CM120 microscope) or a Gatan US1000 CCD (T12 microscope) cameras with the DigitalMicrograph software package.

3. Results and Discussion

3.1. Some Key Visual Observations at 25 °C. The 1000 ppm DPPC dispersions in water, when sonicated as described in Section 2.2, were completely clear and transparent, with no particles visible by eye or in the light microscope. The dispersions were quite stable with time for at least 1 month. The 750 ppm FB solutions in water were cloudy and unstable, and large amounts of large white precipitates were seen. Some particulates flocculated and settled with time. When a stable DPPC dispersion was mixed with an unstable FB dispersion in water, the 750 ppm/1000 ppm FB/DPPC mixture became translucent/bluish, with no visible particles, and it was stable with time, with no precipitates. Thus, we inferred that DPPC vesicles bind to the FB molecules, produced by dissociating FB aggregates which appear to form reversibly, and produce smaller FB/DPPC aggregates which do not settle.

Although the sonicated DPPC dispersions show similar stability in buffer as in water, FB dispersions in buffer behave quite differently, being completely clear, transparent, and quite stable for days and weeks. When a stable FB solution was mixed with a stable DPPC dispersion in buffer, the FB/DPPC mixtures became

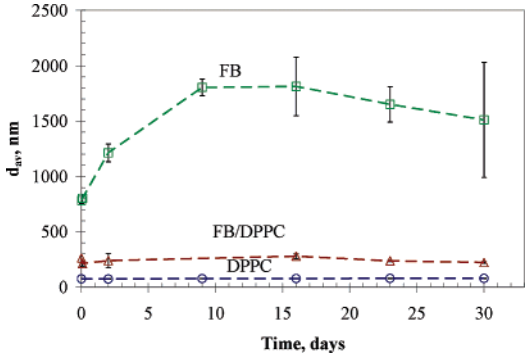

Figure 1. DLS results of average diameter of dispersed DPPC particles, FB molecules or aggregates, and particles of FB/DPPC mixture in water at 25 °C, at various times after preparation: (○) 1000 ppm DPPC; (□) 750 ppm FB; (△) 750 ppm FB/1000 ppm DPPC mixture.

turbid/milky within minutes. Later, they formed flocs which eventually precipitated. This seems to be a typical heterocoagulation behavior, suggesting strong binding between DPPC vesicles and FB molecules, in fact stronger than in water. Thus, even though FB and DPPC do not bind at the air/aqueous interface,[13,14] they do bind in aqueous solution. Apparently, the intermolecular forces are different with different bulk phases (aqueous/aqueous vs air/aqueous), and curvature differences may also play a role.

Since FB, as received, contains 10% citrate, one wonders whether the citrate plays a role in the FB instability in water and stability in buffer. To test this issue, the following experiments were done (see Section 2.2). A 750 ppm FB dispersion in water was dialyzed against water to remove the citrate and the salt present. After 3 and 24 h of dialysis, the dispersion was observed visually and its turbidity was also measured. It was found, as reported previously,[62] that the FB was even more unstable, precipitating faster than without dialysis. The turbidity (values not reported here) was even higher. We infer that FB in water is unstable with or without citrate present.

To test this issue in buffer and also to test the reversibility of aggregation of FB in water and buffer, the following experiments were done. After an FB solution was prepared in water and aggregated, the salts to form the buffer were added. The resulting mixture quickly became clear, indicating that the FB aggregates redissolved. The same behavior was observed when the FB dispersion in water was dialyzed first. We infer (i) that the FB aggregation in water is reversed by salt/buffer (ii) that removing the citrate by dialysis does not alter this conclusion, and (iii) FB is also stable after the citrate is removed.

3.2. DLS Results. The average diameter (d_{av}), the range of the diameters (d-range), and certain Gaussian size distributions of the dispersed particles in 750 ppm FB and 1000 ppm DPPC/ 750 ppm FB mixture in water or buffer are shown in Table 1 and Figures 1 and 2. For DPPC dispersions in water, the average dispersed vesicles diameter was 80 nm (Figure 1).[15] These values remained essentially unchanged for 30 days or more. These DPPC dispersions are quite stable.[13−15]

In water, the average hydrodynamic diameter of FB particles was initially quite high, about 800 nm, which is much larger than the individual FB molecule size (d_h = 18 nm), with a wide distribution from 20 to 1550 nm. With time, the averages increased and the distributions became wider (see Table 1 and Supporting Information). There were definitely even larger particles, not

(61) Talmon, Y. In *Modern Characterization Methods of Surfactants Systems*; Binks, B. P., Ed.; Modern Dekker: New York, 1999; p 147.

(62) Hernandez, E. M.; Franses, E. I. *Colloids Surf., A.* **2003**, *214*, 249.

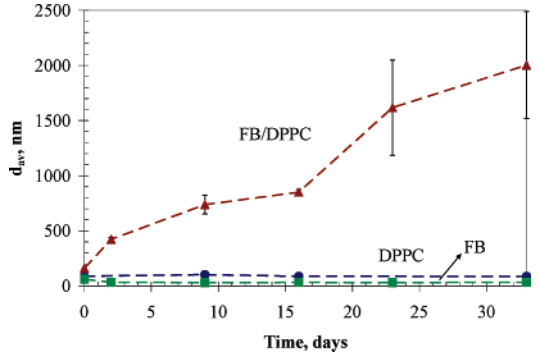

Figure 2. DLS results of average diameter of dispersed DPPC particles, FB molecules or aggregates, and particles of FB/DPPC mixture in buffer at 25 °C at various times after preparation; (●) 1000 ppm DPPC; (■) 750 ppm FB; (▲) 750 ppm FB/1000 ppm DPPC mixture. The abrupt apparent increase of d_{av} at 23 days may be due to effects of aggregates settling and redispersion.

detected by DLS but inferred from the presence of the precipitates. Thus, FB is not stable in water, forms large aggregates, and eventually visible particles which precipitate. Samples were shaken and homogenized before each measurement. The large variations and the decrease in size after 16 days may be due to breaking of some flocculated and settled aggregates caused by the shaking.

For FB/DPPC mixtures in water, the average diameter was 260 nm and the *d*-range was 10−520 nm. The sizes were smaller than those for FB alone but higher than those for DPPC alone. There were few or no significant changes for 30 days (Table 1). Thus, DPPC particles appear capable of causing the FB aggregates to dissociate and, to an extent, stabilize FB against precipitation. We infer that limited size aggregates of lipid particles/protein form in water at 25 °C. This phenomenon has not been reported previously, to our knowledge.

In buffer, the d_{av} value for a 1000 ppm DPPC dispersion was 90 nm (Figure 2)[15] and the *d*-range was 15−160 nm, as reported in a separate article.[15] These values remained almost the same with time, as in water. Hence, these DPPC dispersions in buffer at 25 °C are also quite stable.

The d_{av} value in buffer was 61 nm for a freshly prepared FB solution, it even decreased to 34 nm after 2 days and then remained nearly unchanged for over 1 month. The *d*-range was initially 5−133 nm, then became narrower to 5−70 nm, and later remained unchanged (Table 1, and Supporting Information Figure S2A). The initial size decrease was reproducible and may be due to initially incomplete dissolution of FB. This result demonstrates that FB dissolves in buffer and is quite stable. Some turbidimetry results are presented in Section 3.3.

For FB/DPPC mixtures in buffer, the d_{av} values were around 160 nm, which is much larger than those of DPPC or FB alone, and then increased to over 2000 nm after 1 month (Figure 2), with visible flocculation and precipitation. The abrupt apparent increase of d_{av} at 23 days may be due to effects of aggregates settling and redispersing. The *d*-range was initially 10−310 nm and became much broader, to 5−4000 nm (Table 1 and Figure 4B). Hence, the addition of DPPC vesicles into the stable FB solution in buffer produces quite unstable dispersions with massive floc-like aggregation and precipitation.

3.3. Spectroturbidimetry Results. This method was used to further probe the particle sizes of FB and its mixtures with DPPC. The absorbances *A*, due to scattering alone, at 500 and 380 nm for FB or FB/DPPC mixture are reported in Table 2 and Figure 3.

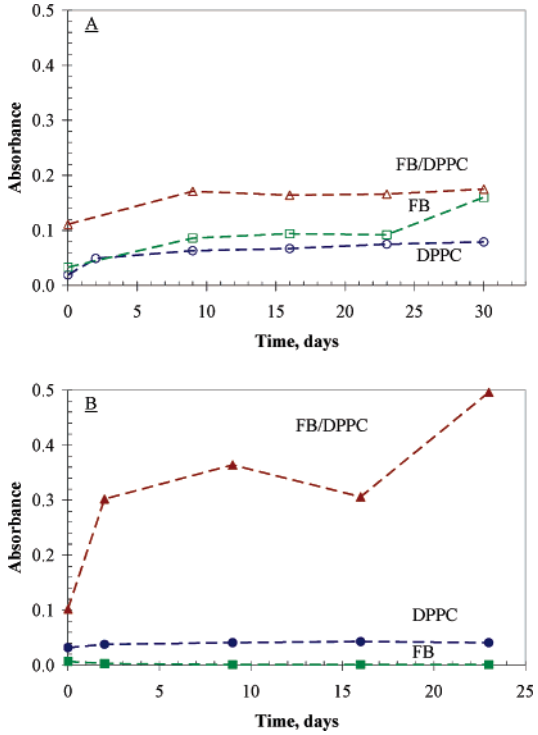

Figure 3. Absorbances at 500 nm of aqueous DPPC, FB, and FB/DPPC mixture: (A) in water; (B) in buffer; (○,●) 1000 ppm DPPC; (□,■) 750 ppm FB; (△,▲) 750 ppm FB/1000 ppm DPPC mixture.

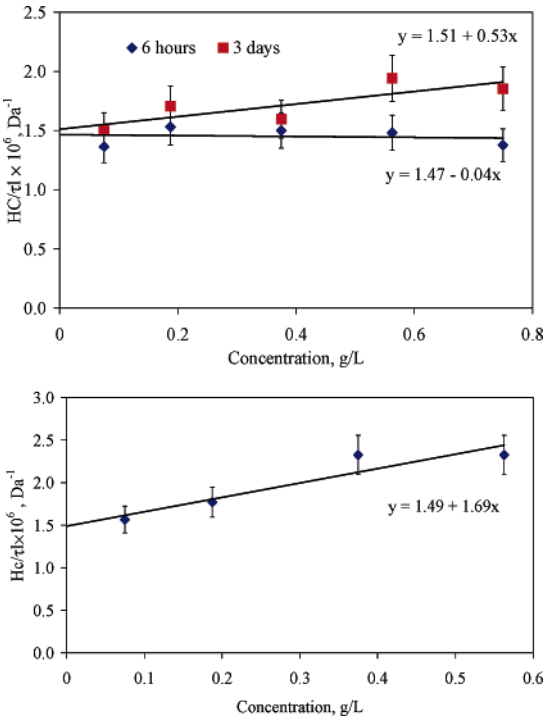

Figure 4. Plot of $Hc/\tau I \times 10^6$ versus *c* for FB in buffer at 390 nm: top, 20 °C, 6 h or 3 days old samples; bottom, 37 °C, 3 h old sample.

At $\lambda = 500$ nm, the absorbance for the DPPC dispersions in water increased only slightly with time (Figure 3A), indicating that the dispersions are quite stable as inferred from the DLS results. The same result was obtained at 380 nm.

For FB in water, some material flocculated and settled with time. The absorbance at 500 nm for FB solution in water increased 5-fold after 1 month, indicating that the solution was somewhat unstable (Figure 3A). The wavelength exponent *g* decreased

Table 2. Data of Absorbances at 500 or 380 nm of Aqueous FB Solution and FB/DPPC Mixture in Water or in Buffer and Average Particle Sizes Estimated from the Wavelength Dependence Exponent *g*

	750 ppm FB				750 ppm FB/ 1000 ppm DPPC			
time, days	A (500 nm)	A (380 nm)	g[a]	$\bar{d}$[b], nm	A (500 nm)	A (380 nm)	g[a]	$\bar{d}$[b], nm
				In Water				
0[c]	0.033	0.068	2.63	159	0.111	0.231	2.67	156
9	0.086	0.122	1.27	1341	0.171	0.299	2.04	517
16	0.094	0.137	1.37	1258	0.164	0.313	2.36	303
23	0.092	0.131	1.29	1332	0.166	0.335	2.56	166
30	0.160	0.109	1.39	1232	0.175	0.365	2.68	155
				In Buffer				
0[c]	0.007	0.009	N/A	N/A	0.102	0.214	2.70	153
2	0.003	0.005	N/A	N/A	0.302	0.520	1.98	610
9	0.001	0.001	N/A	N/A	0.364	0.580	1.70	929
16	0.001	0.004	N/A	N/A	0.306	0.490	1.72	912
23	0.001	0.005	N/A	N/A	0.496	0.731	1.41	1220

[a] Average slope of log A vs log λ_o, where A is the absorbance and λ_o is the wavelength. [b] Diameter d estimated from Mie's theory using tables of Heller et al.[56] for $m = n_p/n_w = 1.10$. [c] Measurements were taken for the freshly prepared sample within 0.5 h.

from 2.6 to ca. 1.3−1.4 (Table 2). The inferred particle size increased from 160 to about 1300 nm, indicating again the FB aggregation, consistent with the DLS results. The differences in the estimated average sizes in the two methods are not unexpected if one considers the wide size distribution of the particles and the assumptions made for the refractive index and the shape of the FB aggregates (compact spherical), even though the shape may be highly nonspherical.

For FB/DPPC mixtures in water, the absorbance at 500 nm remained essentially unchanged with time. The estimated particle size was in the range from 150 to 500 nm. This result indicates that the addition of a stable DPPC dispersion into an unstable aqueous FB dispersion results in a somewhat stable FB/DPPC mixture of particles larger than vesicles, consistent with the DLS results, but smaller than the precipitating aggregates.

In buffer, the absorbance at 500 nm for DPPC dispersions changed little with time (Figure 3B). The absorbance of FB in buffer was about the same as that of the pure buffer ($A < 0.010$), which means that the particle sizes were too small for the g-method to be used accurately.

By contrast to FB in buffer and DPPC in buffer alone, mixtures of FB and DPPC became turbid with visible precipitates, inferred to be lipid−protein aggregates. The absorbance increased significantly with time. The exponent g decreased from 2.7 to 1.4 after 1 month, and the average estimated particle sizes increased from 153 to 1220 nm. Thus, in buffer stable DPPC particles and FB molecules show a strong heterocoagulation effect.

To probe further for the state of FB in phosphate-saline buffer, the absorbances were measured using a more sensitive spectrophotometer, as described in Section 2.4 and as detailed in a previous article.[60] In this procedure the quantity $Hc/\tau I$ is plotted vs c and is extrapolated to $c \rightarrow 0$. Using eq 5, we determined the average molecular weight $\bar{M}_w$ of the protein entities, and the second virial coefficient B (Figure 4). Surprisingly, we found $\bar{M}_w = 680$ kDa, which is twice the FB molecular weight (of the two subunits;[63] see Section 1), both at 20 and 37 °C, for 6 h or 3 days after the solution preparation. This indicates that the FB contains dimeric species on average. This information is novel. It remains unknown whether FB in physiological plasma is also in dimeric form. The physiological significance, if any, of such dimerization is beyond the scope of this article. The possible significance of the second virial coefficients (mostly slightly repulsive) is also not discussed further. Okubo et al., using size exclusion chromatography analysis,[64] reported in 1984 about 10% FB dimers and 90% monomers. Our results show 100% dimers, on average. We have the following hypothesis to explain this apparent discrepancy. When a small pulse of physically aggregated dimers or other aggregates passes through a size exclusion chromatography column, the aggregates are diluted and tend to re-equilibrate with monomers. Then, more monomers may form, and two peaks are observed.[65] The percentage of dimers at the output of the chromatography column may be quite different from that at the original sample. More work is needed with spectroturbidimetry and chromatography to make our explanation definitive.

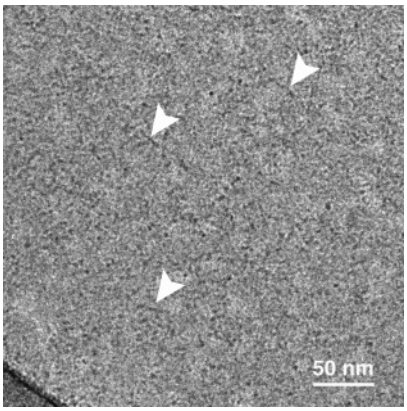

Figure 5. Cryo-transmission electron microscopy (cryo-TEM) images of 375 ppm FB in buffer vitrified from 25 °C. The arrows show FB molecules as clusters of dots.

3.4. Cryo-TEM Results. To probe further the state of FB, a 375 ppm FB in buffer (the concentration was chosen for high sensitivity with no much overlap of molecules in the image) was vitrified from 25 °C and examined by cryo-TEM (Figure 5). The arrows show FB molecules as clusters of dots. Indeed, many large dark dotlike objects are seen. We attribute these to the thrombin nodules of the FB trinodular structure. Although superposition and noise make it difficult to clearly identify the three-dot image of FB,[16−23] the results show clearly no significant aggregation in solution. Although one cannot tell from the images whether pairs of two adjacent molecules are aggregated or not, cryo-TEM supports qualitatively the spectroturbidimetry results

(63) Doolittle, R. F. *Annu. Rev. Biochem.* **1984**, *53*, 195.

(64) Okubo, M.; Azuma, I.; Hattori, H. *J. Appl. Polym. Sci.* **1992**, *45*, 245.

(65) Yu, C. M.; Mun, S.; Wang, N. H. L. *J. Chromatogr.* **2006**, *1132*, 99.

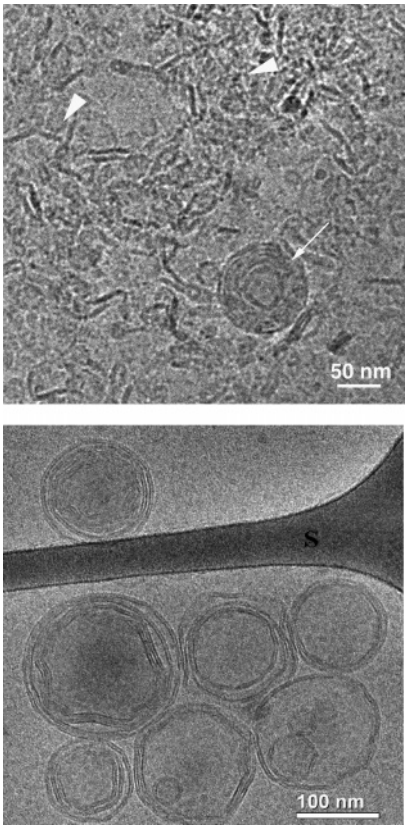

Figure 6. Cryo-TEM images, of top, 250 ppm DPPC/ 188 ppm FB in buffer vitrified from 25 °C. Many aggregates of small vesicles, liposomes (arrow), and membrane fragments (arrowheads) are observed. These aggregates are held together with FB molecules.; bottom, 1000 ppm DPPC in buffer vitrified from 25 °C. Spherical-like objects and no fragments are observed. 'S' denotes the support film.

(Section 3.3). Moreover, the dark dot images can be used to distinguish the protein from the lipid, as discussed below.

A 250 ppm DPPC/188 ppm FB mixture in buffer was vitrified from 25 °C and was examined by cryo-TEM to determine the microstructure of the lipid−protein aggregates (Figure 6, top). Aggregates of small vesicles with FB nodules on their surface (arrowheads) and of liposomes (arrow) apparently bound to many molecules of FB can be seen in the micrograph. Surprisingly, some lipid bilayer membrane fragments bound to FB were also seen. Such fragments were not observed in DPPC vesicles alone; see Figure 6, bottom, and ref 15. These observations are novel. Apparently, as some FB molecules (or dimers) bind to the DPPC vesicles, they cause vesicle breakup and formation of fragments, in addition to DPPC−FB aggregates. Such phenomena of destruction of vesicles by plasma proteins have been inferred indirectly by observing the release of encapsulated solutes[36−39] but without direct cryo-TEM evidence. A schematic representation of the state of aggregation in water and buffer, as inferred from all the available results, is now shown in Figure 7. Some preliminary work on measurements of ζ potentials showed the following FB in water has a net negative charge with ζ potentials of −19 to −12 mV, FB in buffer showed generally variable ζ potentials between −17 and −9 mV. These results do not provide a clear, DLVO-type, explanation of the stability/instability of FB in water or buffer except to confirm the expectation that FB has a net negative charge. More work, and possibly more elaborate theoretical analysis, is needed. The binding of DPPC and FB could be due to electrostatic attraction of the DPPC vesicles, which are zwitterionic but with positive charges outside

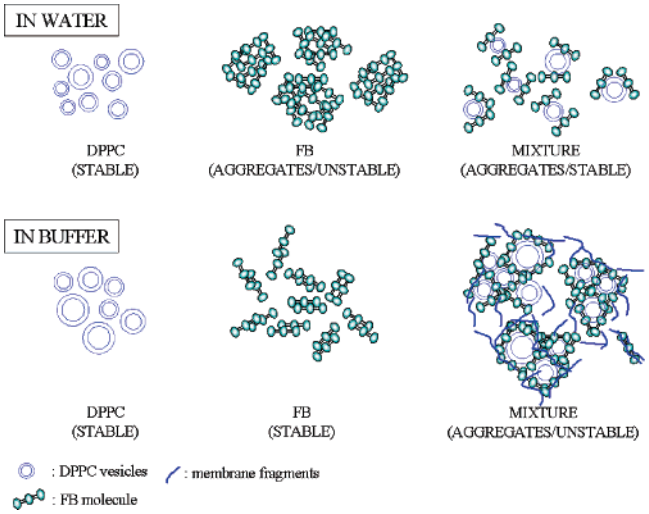

Figure 7. Schematic diagrams of dispersed DPPC, FB, or FB/DPPC particles in water or buffer: each DPPC dispersion is stable with time; the sizes of the dispersed particles are in the range of vesicles in water or buffer. The FB solution in water is unstable, with significant increase in aggregate size with time, but it is stable in buffer. The addition of DPPC in water tends to reverse FB aggregation and produces limited-size lipid/protein aggregates. In buffer, addition of DPPC causes massive unlimited-size aggregation of vesicles with FB molecules and precipitation of flocs. In addition, in buffer some vesicle fragments bound to FB molecules were detected.

($N(CH_3)_3^+$), with some negatively charged groups at the protein surface. In water, the limited heterocoagulation of DPPC and FB can be accounted for, with some charge screening due to the low ionic strength. At high ionic strength, at buffer conditions, the positively charged DPPC vesicles can interact strongly with the negatively charged FB molecules. Evidently, the electrostatic screening is diminished. Hence, a DLVO-type electrostatic destabilization is a plausible mechanism for the heterocoagulation in buffer. More work is needed to quantify the above postulated interactions and confirm this hypothesis.

4. Conclusions

The stability and state of aggregation of FB and DPPC in water or buffer at 25 °C were studied by characterizing the aggregates sizes and morphology with DLS, spectroturbidimetry, and cryo-TEM. Schematic diagrams of dispersed particles in DPPC, FB, or FB/DPPC mixtures in water or buffer are shown in Figure 7. In water, DPPC dispersions are quite stable and contain mostly vesicles. FB solutions in water are quite unstable with significant increases in aggregate sizes with time. The mixing of a stable DPPC dispersion with a quite unstable FB solution in water causes the FB aggregates to dissociate, and produces somewhat stable limited-size, 200−300 nm, particles inferred to be lipid vesicle/protein aggregates. DPPC dispersions in buffer are quite stable with sizes in the 50−100 nm range. FB solutions in buffer are also quite stable, and FB forms small dimers with sizes of about 30 nm (cf. to the hydrodynamic size of 18 nm for single FB molecules). FB aggregates form in water also when the citrate is removed by dialysis. The FB aggregation in water is reversed when salts are added to form the buffer. Hence, the FB solution in buffer appears to be in an equilibrium state. The addition of a stable DPPC dispersion into a stable FB solution in buffer causes the formation of massive lipid−protein floc-like aggregates, many of which precipitate. These results have implications in understanding lipid/protein interactions, which are important in biological applications such as biosensors, in

elucidating liposome stability in serum, in food processing, and in lung surfactants inhibition by serum proteins.

Acknowledgment. This research was supported by the National Science Foundation (Grant No. CTS 0457289). We thank Prof. Y-.Y. Won for allowing the use of the dynamic light scattering instrument. We also thank Prof. J. A. Morgan for allowing the use of a UV−vis spectrophotometer. The cryo-TEM work was performed at the Hannah and George Krumholz Laboratory for Advanced Microscopy, part of the "Technion Project on Complex Fluids, Microstructure and Macromolecules".

Supporting Information Available: Two figures showing the time dependence of the particles size distribution from DLS; see also Table 1. This material is available free of charge via the Internet at http://pubs.acs.org.

LA0634701